ACS APPLIED MATERIALS & INTERFACES

Research Article

www.acsami.org

New Method for Super Hydrophobic Treatment of Gas Diffusion Layers for Proton Exchange Membrane Fuel Cells Using Electrochemical Reduction of Diazonium Salts

Yohann R. J. Thomas,* Anass Benayad,* Maxime Schroder, Arnaud Morin, and Joël Pauchet

Commissariat à l'Energie Atomique de Grenoble, 17 rue des Martyrs, 38054 Grenoble Cedex 9, France

ABSTRACT: The purpose of this article is to report a new method for the surface functionalization of commercially available gas diffusion layers (GDLs) by the electrochemical reduction of diazonium salt containing hydrophobic functional groups. The method results in superhydrophobic GDLs, over a large area, without pore blocking. An X-ray photoelectron spectroscopy study based on core level spectra and chemical mapping has demonstrated the successful grafting route, resulting in a homogeneous distribution of the covalently bonded hydrophobic molecules on the surface of the GDL fibers. The result was corroborated by contact angle measurement, showing similar hydrophobicity between the grafted and PTFE-modified GDLs. The electrochemically modified GDLs were tested in proton exchange membrane fuel cells under automotive, wet, and dry conditions and demonstrated improved performance over traditional GDLs.

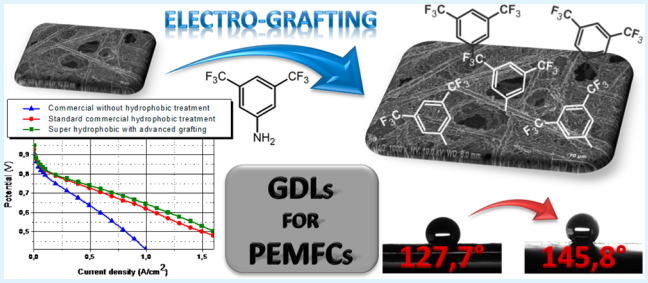

KEYWORDS: *fuel cells, GDL, hydrophobicity, water management, diazonium, grafting*

1. INTRODUCTION

Fuel cell technology is one of the most studied academic and industrial fields linked to energy production. However, the complex phenomena involved when fuel cells are running are still being investigated in order to develop superior technological solutions that will increase performance. For example, one important area of study includes water management in PEMFCs with particular emphasis on flooding phenomena.[1] Water produced at the cathode side of a PEM fuel cell is generated by oxygen reduction reaction (ORR) and by humidification of gases to ensure sufficient hydration of the membrane.[2] The competition between both water generation processes may contribute to the mass transport loss through pore blockage by liquid water, catalyst site flooding, and the decrease of oxygen concentration near active catalytic sites.[3,4] Several solutions have been proposed to control flooding-related consequences by targeting specific modifications to fuel cell components in order to improve electrochemical performance.[5]

In the case of GDLs, usually made of porous carbon paper or carbon cloth, known as wet-proofed, several hydrophobic agents have been added to prevent the flooding process. The previous research recorded GDLs treated with CF_4 plasma,[6] perfluoroalkoxy (PFA),[7] perfluoropolyether (PFPE),[7−9] poly(vinylidene fluoride) (PVDF),[10,11] fluorinated ethylene propylene (FEP),[7,12,13] and silicone nanolayer,[14] and the most widely used is poly(tetrafluoroethylene) (PTFE).[15−21] Different commercial GDLs were developed to respond to commercial specification[22,23] to answer customized demand in terms of various operating conditions such as stationary and automotive. In this respect, PTFE prepared by GDL immersion in an emulsion containing the hydrophobic agent, drying, and sintering at 350 °C is the most commonly used technology.[16,18]

However, the fine-tuning of these properties depends on the ability to balance the hydrophobic and hydrophilic properties of GDLs. For example, in the case of PTFE treatment, the GDL will exhibit mixed wettability due to both the hydrophobic agent and hydrophilic carbon fibers network,[24] directly impacting liquid water transport and mass transport losses. Sinha and Wang[24] demonstrated, based on a pore-network model, that liquid water will preferentially flow through connected GDL hydrophilic networks, which could be responsible for the flooding of pores. Pore network simulations have shown that, as hydrophilic pore ratio increases, gas diffusion will decrease[25] and performance of PEMFC will decline.[26]

Therefore, the fraction of hydrophilic pores is a key parameter for mass transport losses, a criterion for an optimum content of PTFE.[16,18,19,21] In other words, an abundance of hydrophobic agent will cause a decrease in porosity and gas diffusion leading to a decrease of mass transport.[27] Other works have shown that the wettability of the surface of GDL increased by 10 wt % PTFE, but the contact angle measurements remained constant with further increases of PTFE concentration, up to 40 wt %.[12,28] Moreover, it has been shown that the content of hydrophobic agents in the GDL cannot account

Received: May 22, 2015
Accepted: June 22, 2015
Published: June 22, 2015

DOI: 10.1021/acsami.5b04428
ACS Appl. Mater. Interfaces 2015, 7, 15068−15077

entirely for the transport of liquid water through the GDL. However, the distribution of PTFE will have a major impact on water transport.[29] Scanning electron microscopy (SEM) coupled with energy-dispersive X-ray spectroscopy (EDS), performed on cross sections of commercial GDLs, demonstrated that the breakdown of PTFE across the thickness of GDL is heterogeneous[30] and that fluorine was more concentrated at the external surfaces of the GDLs. Ito et al.[31] revealed that the PTFE distribution strongly depends on the drying process used in hydrophobic treatments, by demonstrating that under atmospheric pressure the traditional drying processes produced a more heterogeneous material compared to vacuum drying. This heterogeneity can lead to uncoated areas of gas fibers preventing droplet removal, as was recently simulated by Molaeimanesh et al.[32]

An alternative means of making GDL hydrophobic is grafting diazonium salts which are widely used in many applications such as energy storage systems[33] or improvement of membrane selectivity,[34] thus paving the way toward the controllability of local chemical properties. Grafting has been performed onto metallic surfaces such as iron[35−37] or gold,[38−40] carbon materials like carbon nanotubes,[41] glassy carbon,[35] carbon blacks,[42−44] carbon films,[45] graphite,[46,47] carbon felts,[48] and other nonconductive surfaces like polymers.[49]

Using this method, aryl diazonium offers a wide variety of functionalities such as nitro,[35,39,47,50−52] carboxyl,[36,40] alkyl,[37] halogeno,[37] amino,[38,39,53−57] trifluoromethyl,[42] sulfonic,[42,43] or thiol[46] groups. Since two principal methods are used to covalently bond molecules to the surface (either reaction of the amine in organic media[41] or in situ generation of diazonium salt in acid aqueous media[38,55,58]), the simple modulation of the functional group was exploited to control the wettability as well as the transport properties. Grafting could be realized with[59] or without electrochemical control;[60] in this last case, the reaction occurs spontaneously at the material surface. We noted that the electrochemical reduction of diazonium salts is a one-step process through covalent bonding between the carbon surface and the phenyl group, whereas at least two stages are needed for PTFE treatment (immersion of GDL in a PTFE emulsion and then sintering).

In this study, we achieved the hydrophobicity of GDL by grafting organic molecules containing hydrophobic functionalities to the carbon surface through the electrochemical reduction of diazonium salts.[61,62] In particular, electrografting enabled the covalent bonding of hydrophobic molecules at the surface of conductive carbon fibers. With this method, we expected more homogeneous results than PTFE treatment that can be carried out without modifying the structure of the GDL (no reduction of porosity or gas permeability); only a thin layer of molecules was grafted at the surface of the GDL.

The aim of this research project was to improve commercial and mature GDL materials to meet optimal water transport properties. The purpose was twofold: (1) find an optimum grafting method of CF3-containing amines onto glassy carbon; (2) test the GDL grafted with CF3 containing amines in PEM fuel cell under different operating conditions.

A direct comparison between GDLs with grafted phenyl groups containing one or two CF3 functions and PTFE-treated GDLs was performed based on a joint study using electrochemical (fuel cell performances), surface characterization (contact angle and XPS), and SEM (coupled with EDS) performed on cross sections of GDLs. The contact angle and the XPS analyses, based on core level spectra and core level mapping, allowed us to confirm the homogeneity and the efficiency of such hydrophobic treatment for cells operating in automotive, dry, and wet cycling conditions. We demonstrated an improvement of PEM fuel cell performances using hydrophobic CF3-terminated amines compared to those with traditional PTFE.

2. EXPERIMENTAL SECTION

2.1. Modification of Carbon Supports. After a glassy carbon (GC) electrode of 3 mm diameter (Bioanalytical Systems Inc.) was polished and rinsed with ultrapure water (Milli-Q water 18.2 MΩ cm, Direct-Q 3, Millipore), its electrochemical modification was carried out in a standard three-electrodes setup. The GC was used as the working electrode, and a mercury/mercurous sulfate (Hg/Hg_2SO_4) was used as the reference electrode (Bioanalytical Systems Inc., RE-2C) along with a platinum wire used as the counter electrode. Electrochemical measurements were performed with a BioLogic, VMP2 potentiostat. The grafting onto GDLs was conducted based on the same setup with the only difference being the choice of a larger size counter electrode and the working electrode; both were hydrophilic GDLs.

The two-stage grafting process is reported in Figure 1a and b. First the diazonium salt precursors are in situ generated in an acid medium

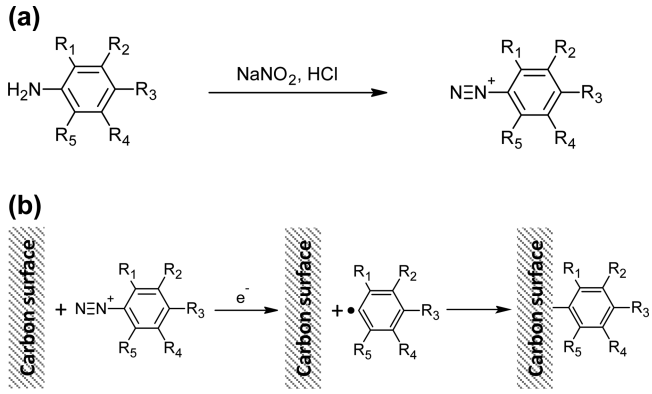

Figure 1. (a) In-situ generation of diazonium salts. (b) Grafting onto carbon surface under potential cycling.

with sodium nitrite as an oxidant (Figure 1a) from the amine precursor. Then, the grafting of diazonium molecules with functional groups on the carbon surface was carried out under electrochemical potential cycling control (Figure 1b).

With regards to searching for hydrophobic properties, we acted on the functional R1−R5 groups in the diazonium salt. For our study, we targeted the following hydrophobic functionalities R1 = R2 = R4 = R5 = H, R3 = CF_3, and R1 = R3 = R5 = H, R2 = R4 = CF_3, respectively. Two reagents from Sigma-Aldrich were used, 4-(trifluoromethyl)-aniline (named 1CF3), and 3,5-bis(trifluoromethyl)aniline (named 2CF3). All reagents were used, as received, dissolved in aqueous solutions of 0.5 M HCl containing sodium nitrite ($NaNO_2$) using the protocol described by Baranton et al.[58]

The reduction of diazonium salts was realized by a linear negative variation of potential (50 mV/s scan rate) between +0.2 and −1.0 V vs Hg/Hg_2SO_4. Since we observed no significant variation of current after 30 cycles, we chose to perform some additional cycles (for a total of 50 cycles) in order to be certain to obtain a complete grafting onto the carbon surface. After grafting, the material was carefully rinsed with ultrapure water several times.

The presence of the grafted material was studied by cyclic voltammetry at 50 mV/s from +0.2 to −0.6 V vs Hg/Hg_2SO_4 in a KCl 0.1 M solution with ferro/ferricyanide $[Fe(CN)_6]^{4-}/[Fe(CN)_6]^{3-}$ (both compounds at a concentration of 5 mM), which is commonly used in electrochemistry due to its high sensitivity to the state of the surface.[63] Based on our results, it is possible to determine if

DOI: 10.1021/acsami.5b04428
ACS Appl. Mater. Interfaces 2015, 7, 15068−15077

the surface has been blocked, indicating whether grafting has occurred or not.

Once optimal parameters were determined, the same grafting procedure was performed onto a GDL without any hydrophobic treatment (labeled AA). The GDLs were obtained from SGL Group (Sigracet GDL 24 series) which has proven to be one of the best sources available in the PEMFC market. We obtained two hydrophobic GDLs labeled AA-1CF3 and AA-2CF3.

For comparison, a commercial GDL with hydrophobic PTFE treatment was used and labeled BA (same material as AA but with 5 wt % PTFE treatment) and BC (same material as BA but with a microporous layer). A self-supported homemade microporous layer (MPL) was added to all GDLs except for BC. MPL is a thin porous layer sandwiched between the GDL and the active layer made of carbon nanoparticles which are mixed with a hydrophobic agent. Membrane electrode assemblies (MEAs) were obtained by assembling two identical GDLs (with MPL) between a membrane. A summary of different GDLs and MEAs used in this research project is reported in Table 1.

Table 1. Nomenclature of Hydrophobic Agents, GDL, and MEAs Used

hydrophobic agent	GDL	MEA
none	AA	AA/MPL
1CF3	AA-1CF3	AA-1CF3/MPL
2CF3	AA-2CF3	AA-2CF3/MPL
5 wt % PTFE	BA	BA/MPL
5 wt % PTFE + MPL	BC	BC

2.2. Contact Angle Measurements. The contact angle measurements, performed at the surface of the GDLs AA, BA, BC (microporous side), AA-1CF3. and AA-2CF3 were carried out at room temperature with a contact angle analyzer (KRUSS DSA100). The contact angle was estimated as the mean value of five different measurements of 8 μL water droplets onto the different GDL surfaces.

2.3. Energy-Dispersive X-ray Spectroscopy (EDX) Characterization. Analysis of the fluorine breakdown among the GDL thicknesses was carried out by embedding the GDL in an epoxy resin for cross-section observation by a ZEISS-LEO 1530 field emission gun scanning electron microscope (FEG SEM). This FEG SEM is equipped with a Bruker Silicon Drift Detector (SDD) for energy-dispersive X-ray spectroscopy (EDS) analyses. The procedure used was similar to the one reported by Rofaiel et al.[30] The different GDLs were placed in a mold and embedded in a resin under primary vacuum to allow the resin to fill all the pores and avoid trapped air. The resin was cured overnight, and the resulting material was carefully polished prior to being coated with a thin conductive carbon layer since the resin has low electrical conductivity.

2.4. X-ray Photoelectron Spectroscopy (XPS) Characterization. The XPS (VersaProbe-II, ULVAC-Phi), known to be a nondestructive extreme surface analysis, were performed using focused monochromatized Al Kα radiation (1486.6 eV). The spectrometer was calibrated using photoemission lines of gold (Au $4f_{7/2}$ = 83.9 eV, with reference to the Fermi level). The core level peaks were recorded with constant pass energy of 23.3 eV. The XPS spectra were fitted using Multipak V9.1 software in which a Shirly background was assumed and the peak fittings of the experimental spectra were defined by a combination of Gaussian (80%) and Lorentzian (20%) distributions. The XPS chemical mapping was performed in unscanned mode with pass energy of 93 eV. The chemical mapping was statistically treated using linear least-squares fitting.

2.5. MEAs and Single Fuel Cell Tests. MEAs were prepared by assembling a catalyst-coated membrane (CCM) with two identical GDLs for anode and cathode sides. The CCM was achieved with coated catalyst layers with anode (Pt/Vulcan XC 72R catalyst, TEC10 V50E, TKK) and cathode (Pt_3Co/Vulcan XC 72R catalyst, TEC36 V52, TKK) loadings of 150 and 450 $\mu g_{Pt}/cm^2$ respectively. Both were separated by a Nafion HP membrane. A self-supported homemade MPL was added to the surface of the GDL prior to assembly. This was carried out with all GDLs with the exception of BC which already possesses a commercial MPL.

The prepared MEAs were tested in 25 cm^2 single cells with a single serpentine flow field. The width and the depth of the channel was 1.4 mm, and the width of the rib was 0.8 mm. A FuelCon Evaluator-C 70350 bench was used. The tests were carried out at 1.5 bar using humidified hydrogen and air. The hydrogen and air stoichiometries were kept at 1.2 and 2.0 respectively in a counter-flow configuration.

The prepared MEA was broken-in until stable performances were obtained. Three different experimental conditions were performed, in the following order, with identical relative humidity (RH) on both the anode and cathode sides:

(1) automotive conditions = 80 °C and 50% RH;

(2) wet conditions = 60 °C and 100% RH for enhanced water flooding;

(3) dry conditions = 80 °C and 20% RH.

3. RESULTS AND DISCUSSION

Cyclic voltammetries of 1CF3 grafting onto GC are represented in Figure 2. During the first potential cycle from

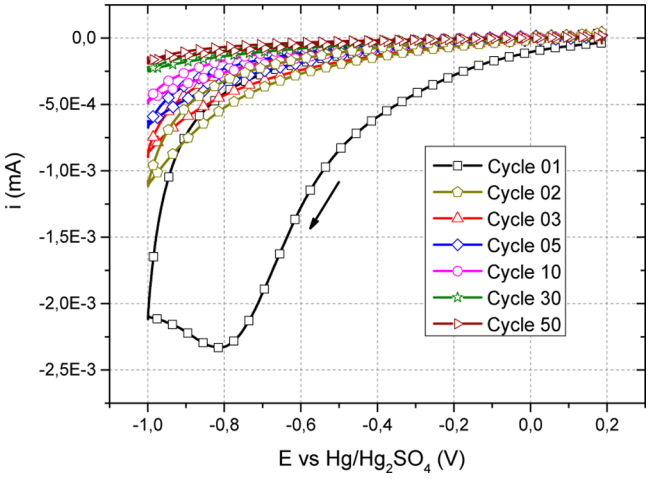

Figure 2. Cyclic voltammetry of 1CF3 diazonium salt (4 mM) onto glassy carbon at 50 mV/s in HCl 0.5 M.

+0.2 to −1.0 V vs Hg/Hg_2SO_4 we observed a peak at −0.82 V corresponding to the reduction potential of diazonium salt.[42] After further potential cycles, the current decreased as the surface was getting partially grafted and had become progressively more saturated.

As mentioned above, measuring the cyclic voltammetry in a solution containing the oxidoreduction compounds $[Fe(CN)_6]^{4-}/[Fe(CN)_6]^{3-}$ is a direct means of characterizing the electrochemical state of the surface. The glassy carbon was studied after three different steps: before grafting, after four cycles, and at the end of the grafting process (50 cycles), as shown in Figure 3.

The cyclic voltammetry of $[Fe(CN)_6]^{4-}/[Fe(CN)_6]^{3-}$ compounds showed a progressive carbon surface blocking, after grafting, the signature of electronic exchange loss at the surface of grafted GC. Indeed, before grafting, the cyclic voltammetry response clearly showed reversible peaks of the redox compounds $[Fe(CN)_6]^{4-}/[Fe(CN)_6]^{3-}$. After four cycles, a clear attenuation of the ferro/ferri cyanide redox-related peaks was observed. After 50 cycles, we noted that the redox peaks completely disappeared within this potential range. This result proved that the grafting process occurred at the

DOI: 10.1021/acsami.5b04428
ACS Appl. Mater. Interfaces 2015, 7, 15068−15077

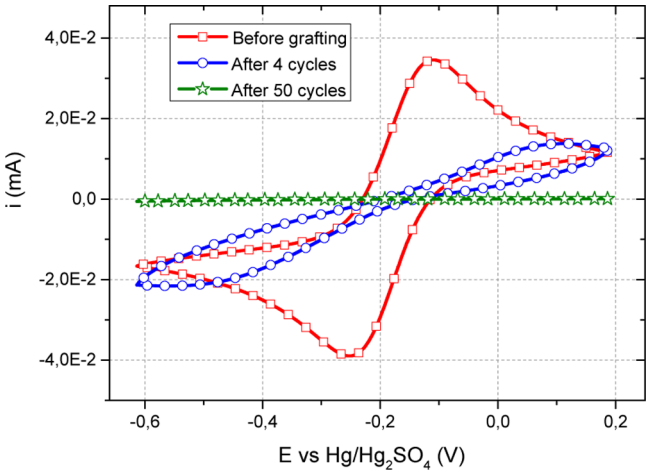

Figure 3. Cyclic voltammetry at 50 mV/s of $[Fe(CN)_6]^{4-}$/$[Fe(CN)_6]^{3-}$ compounds (5 mM) on grafted glassy carbon by 1CF3 in KCl 0.1 M.

surface of the GDLs. We conducted the same procedure for the 2CF3 amine and obtained similar results.

Grafting onto GDL was also achieved with the same grafting procedure used with GC. The GDL of 4 × 5 cm^2 without any hydrophobic treatment (AA) was used and tested with the same ferro/ferri cyanide couple as described above.

The cyclic voltammetry of $[Fe(CN)_6]^{4-}$/$[Fe(CN)_6]^{3-}$ onto GDL AA in Figure 4 showed a similar result as GC grafting.

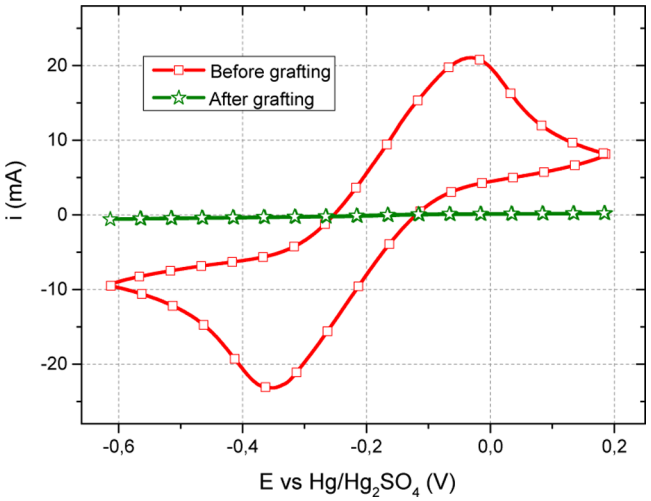

Figure 4. Cyclic voltammetry at 50 mV/s of $[Fe(CN)_6]^{4-}$/$[Fe(CN)_6]^{3-}$ compounds (5 mM) onto GDL AA before and after 50 cycles of 1CF3 grafting in KCl 0.1 M.

After 50 cycles the surface was totally blocked. Grafted molecules imply an increase in transfer resistance charge for the ferro/ferri cyanide compounds as they form a layer at the carbon surface, which acts as a physical barrier for the redox process. The same result was observed for the GDL-labeled AA-2CF3.

To probe the hydrophobicity of our grafted surfaces, we performed a contact angle measurement at the surface of the different GDLs and MPL (in the case of BC) as shown in Figure 5.

The contact angle of GDL (AA) was estimated to be 127.7° and increased to 142.2° and 145.8° for AA-1CF3 and AA-2CF3, respectively. The AA-2CF3 showed the highest contact angle and therefore was the most hydrophobic GDL. This result allowed us to confirm that hydrophobic grafting occurred. The hydrophobicity depends on the number of CF3 groups. In the case of 5 wt % PTFE (BA), we noticed an increase of about 15° compared to AA. This correlates with values reported for the same GDLs with an increase of 13.5, 14.0, and 11° after PTFE treatment of 10, 20, and 30 wt %.[28] It can be noted that there were no significant changes in the contact angle measured on treated carbon papers when the hydrophobic agent was increased higher than 10 wt %. Lim et al.[12] showed a similar trend with FEP loadings from 10 to 40 wt %. Moreover, contact angle values after grafting indicated that our GDLs reached superhydrophobic levels.

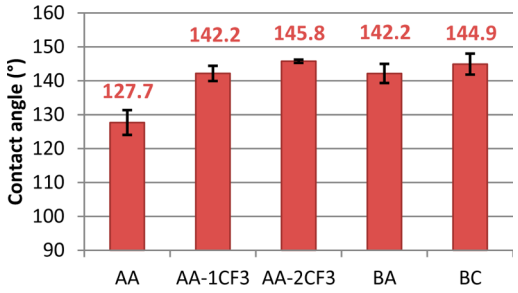

Figure 5. Contact angles of 8 μL water drop onto different carbon surfaces.

As explained by Gurau et al.,[64] the contact angle measured in this case was representative of the wetting phenomena on the external surface of the GDL, which will depend on surface roughness. This explains why the microporous side of BC shows slightly higher hydrophobic behavior compared to BA due to different surface roughness between materials and has also higher contact angle than measured on a PTFE film, which is around 105°.[65] Conversely, the internal contact angle gives indications on the wetting properties of the internal structure, which is something closer to the capillary forces acting on the water at a pore scale. As water has relatively high surface tension (72 mN/m at 25 °C)[66] and fluorinated carbon chains (like CF2 in PTFE) have a lower surface tension (14 mN/m at 23 °C),[67] water will fill principally the hydrophilic pores inside the GDL, which is consistent with contact angle values lower than 90° on highly ordered pyrolytic graphite (HOPG) which is a smooth graphitic material of high purity.[68] It is then hard to reach a conclusion on mass transport or water management based only on external contact angle measurements. Moreover, it has been shown that the contact angle generally decreases when temperature increases,[12] so this measurement may not be representative of the operating conditions inside the PEMFC. Further single fuel cell tests will give information on the capabilities of the material to operate under specific operating conditions.

To probe the bulk fluorine distribution of our grafted GDL, we performed an EDX mapping on the cross section of commercial GDLs BA and BC as reported in Figure 6a and b. Linear fluorine concentration profile across the thickness of GDLs has been added. The EDS imaging shows clearly an heterogeneous breakdown of PTFE through the fluorine signal with higher concentration at the top and bottom surfaces of the GDLs. This result correlates with previous studies.[30,31]

The case of BC is interesting as it shows a more homogeneous breakdown of fluorine inside the MPL (Figure 6b) and, like BA, has higher concentrations of fluorine at the

DOI: 10.1021/acsami.5b04428
ACS Appl. Mater. Interfaces 2015, 7, 15068−15077

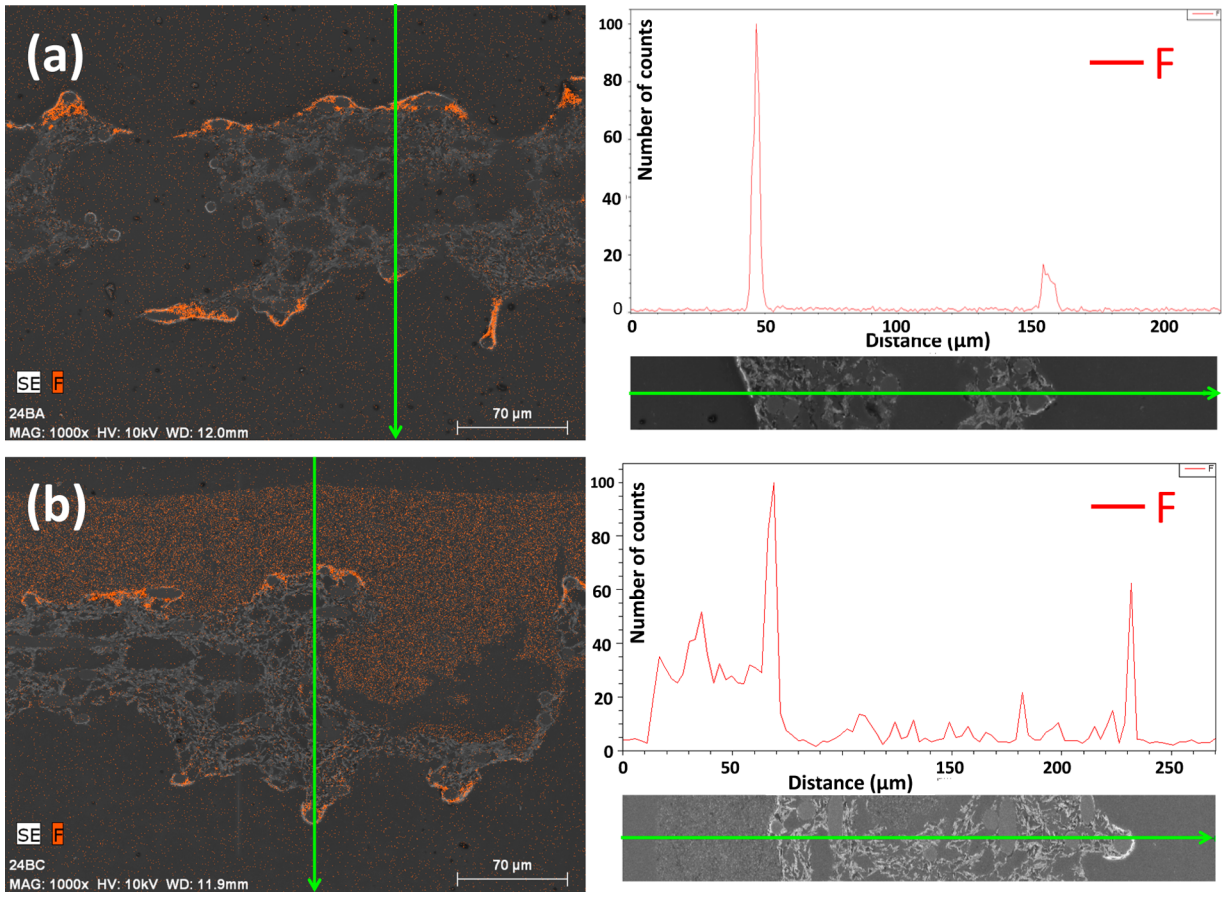

Figure 6. EDS imaging. (a) BA; (b) BC. Left: Secondary electron image and fluorine signal. Right: Fluorine concentration profile across the thickness of the GDLs.

external surfaces of the GDL. However, the EDS analysis performed on AA-1CF3 and AA-2CF3 was not successful due to the low fluorine signal in the grafted compounds. The images obtained were similar to those obtained with AA indicating that the signal recorded basically noise. Therefore, for accurate analysis of the fluorine distribution in grafted GDLs, we performed an XPS analysis.

The electrochemical grafting was investigated by means of XPS, by probing the C 1s and F 1s core level peaks. The C 1s peak registered at the surface of the bare GDL (Figure 7) shows the signature of graphite-like carbon, with the presence of an asymmetric main peak at 284.6 eV, assigned to sp^2/sp^3 carbon hybridization.[69] A large band at higher band energy centered at 290.6 eV is attributed to $\pi-\pi^*$ plasmon peak which is additional proof of the presence of a graphite-like structure. In the case of GDL-labeled AA-1CF3, the C 1s core spectrum shows an additional peak at higher binding energies (292.6 eV), assigned to CF3 bonds. Several peaks were also detected at 285.7, 286.7, 288.1, and 291.2 eV related to sp^3 carbon, carbon bonding to one, two oxygen, and the $\pi-\pi^*$ plasmon band, respectively.[70,71] A similar spectrum was registered at the surface of the GDL-labeled AA-2CF3. The F 1s related spectra of AA-1CF3 and AA-2CF3 are reported in Figure 7. We observed one main symmetric peak at 688.0 eV, assigned to C−F bonds like in Ph−CF3 groups.

Interestingly, we observed in both cases the presence of a band at 694.6 eV. This may be assigned to an interatomic coupling between F 1s photoelectron and the plasmonic π cloud of the grafted phenyl groups. A zoom on this spectral region was given in the inset of the fluorine spectra. In the case of GDL-labeled BA (with PTFE), the C 1s core spectrum shows two intense peaks at 284.6 and 291.9 eV, attributed to graphite-like carbon and C−F bonds in PTFE, respectively. The experimental spectrum is fitted with two additional peaks at 286.8 and 289.0 eV, attributed to C−O and F−C−O/COO bonds, respectively. The corresponding F 1s peak is centered at 689.1 eV.

Semiquantitative analyses based on fluorine atomic percent performed at the surface showed the presence of 18, 27, and 43 at. % for AA-1CF3, AA-2CF3. and BA. respectively (Table 2). The relative atomic concentration of C−F related bonds in the C 1s peak showed 5.1 and 8.1 at. % for AA-1CF3 and AA-2CF3, respectively. This is almost three times the relative atomic concentration of F−C related bonds in F 1s peak and correlates with a structure of one carbon bonded to three fluorine atoms.

Figure 8a and b report the XPS chemical distribution of carbon and fluorine-related bonds (C−C, C−F) at the surface of AA-2CF3 and BA (PTFE) GDLs. The XPS chemical mapping was performed on an area of 300 × 200 μm^2 using the unscanned mode of the spectrometer with an X-ray spot area of 7 × 7 μm^2. A linear least-squares picture fitting was used to improve the signal-to-noise level. The XPS mapping of C−C and C−F bonds indicates a homogeneous fluorine distribution of the hydrophobic phenyl groups at the surface of GDL AA-2CF3. We observed a similar pixel intensity brightness of both bonds, indicating that the grafted molecules covered the entire surface of the fibers. In the case of PTFE-treated GDL, we

DOI: 10.1021/acsami.5b04428
ACS Appl. Mater. Interfaces 2015, 7, 15068−15077

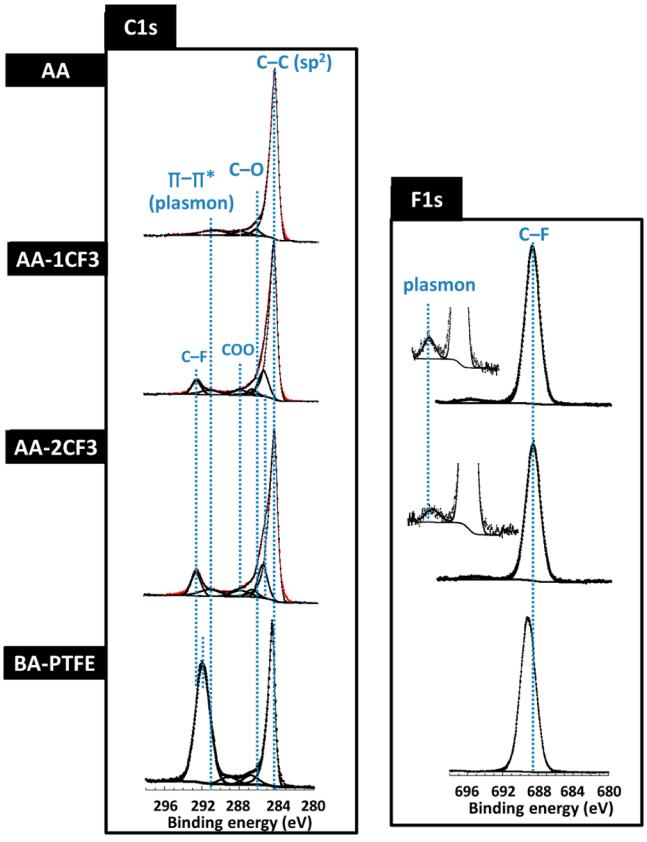

Figure 7. XPS C 1s and F 1s core peaks taken at the surface of the GDLs-labeled AA, AA-1CF3, AA-2CF3, and BA-PTFE.

Table 2. XPS Relative Atomic Concentration of C, O, and F of Different GDLs

	C (at. %)	O (at. %)	F–C (F 1s) (at. %)	C–F (C 1s) (at. %)
AA-1CF3	76	6	18	5.1
AA-2CF3	69	4	27	8.1
BA-PTFE	56	1	43	–

observed that the intensity of fluorine-related bonds (C–F) was slightly higher than the C–C-related intensity owing to the polymeric nature of PTFE, which masked the signal from the carbon fibers (i.e., sp^2-related bonds).

To overcome the resolution limit of XPS mapping (7 × 7 μm^2), we obtained SEM images with an Auger spectrometer. Figure 9 shows a SEM image of the bare GDL, which consists of a mixture of carbon fibers and graphite sheets mixed with binder. We could identify clearly that the pores between carbon fibers were not blocked in the case of the GDL-labeled AA-2CF3, unlike the one treated with PTFE.

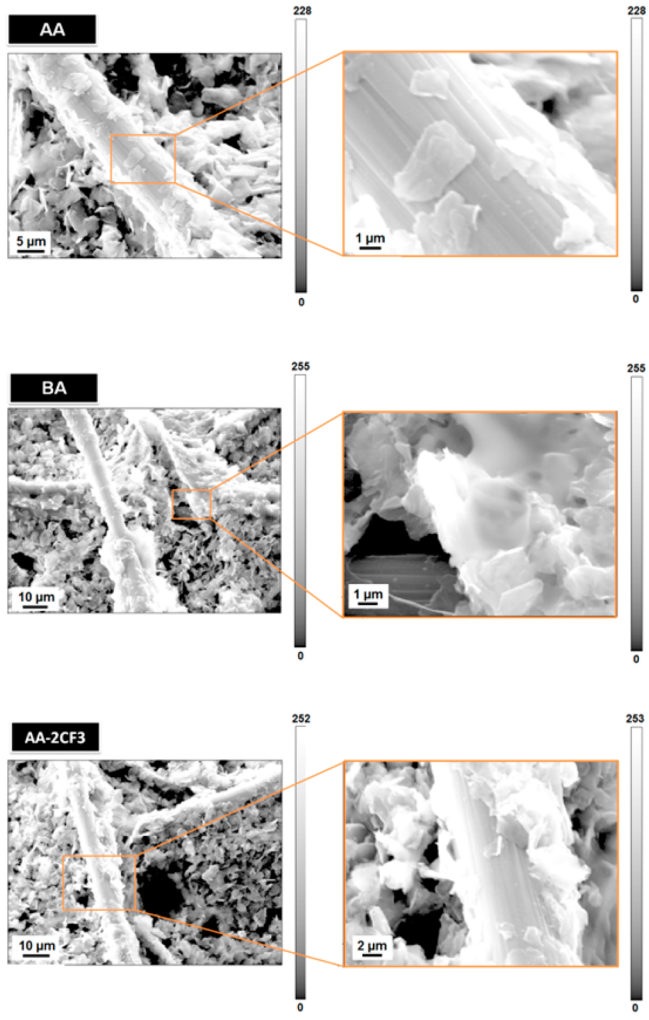

Figure 9. Auger scanning electron microscopy image taken at the surface of GDLs-labeled AA, AA-2CF3, and BA.

Besides the detailed XPS studies, electrochemical analyses were also systematically carried out on different grafted GDLs.

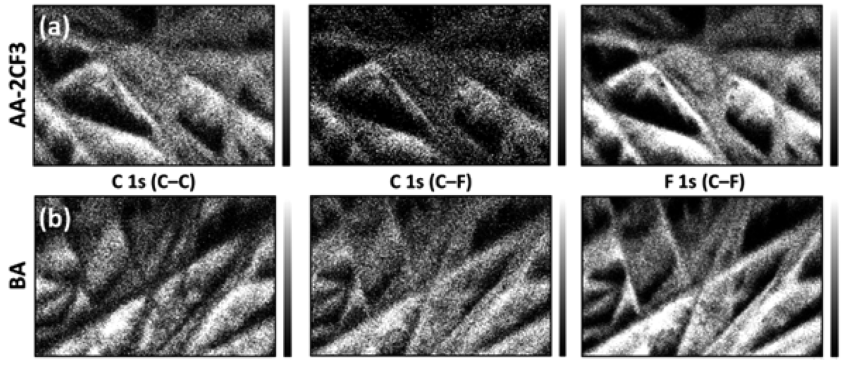

Figure 8. XPS C 1s (C–C), C 1s (C–F), and F 1s (C–F) chemical mapping performed at the surface of (a) AA-2CF3 and (b) BA GDLs. Each picture is 300 × 200 μm^2 pixels (pixel size is 7 × 7 μm^2).

DOI: 10.1021/acsami.5b04428
ACS Appl. Mater. Interfaces 2015, 7, 15068–15077

The polarization and power density curves of different GDLs are reported in Figure 10, Figure 11, and Figure 12 for automotive, wet, and dry conditions, respectively.

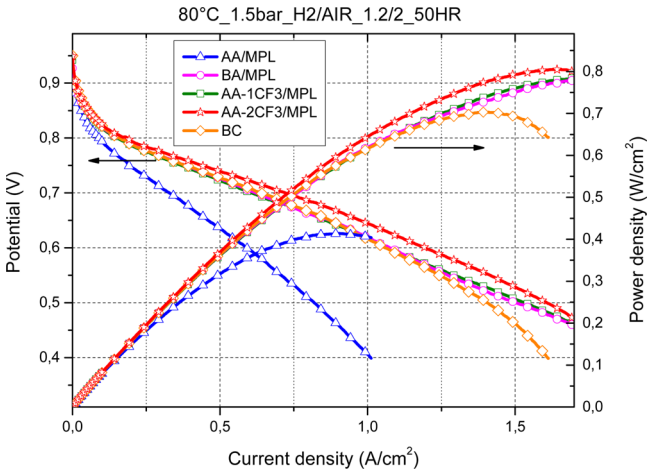

Figure 10. Polarization curves for automotive conditions.

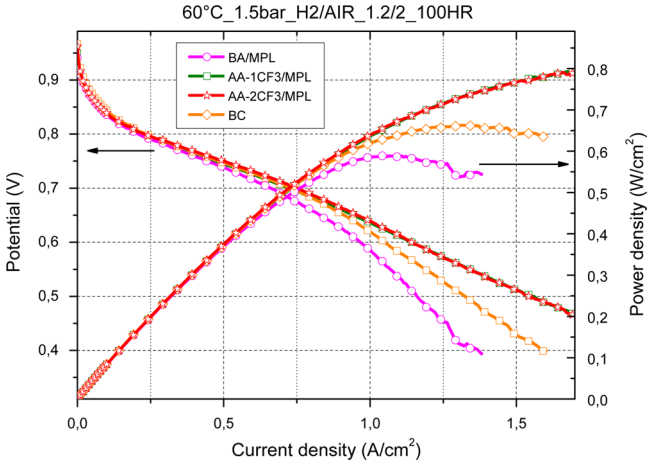

Figure 11. Polarization curves for wet condition.

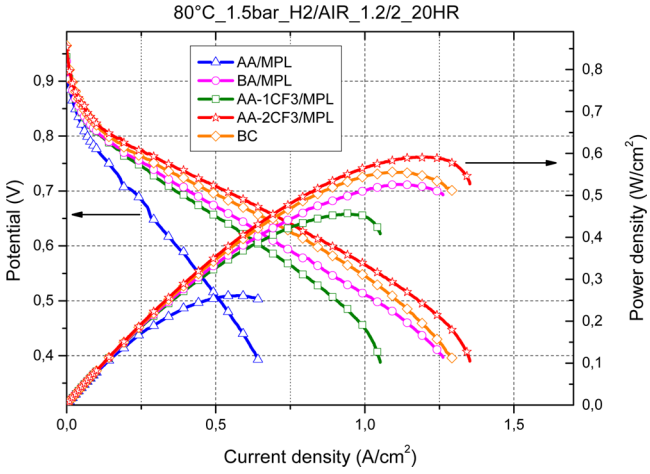

Figure 12. Polarization curves for dry condition.

For automotive operating conditions (Figure 10), in the case of the GDL-labeled AA, the lowest performances were obtained. This confirmed that in those operating conditions, hydrophobic treatment is necessary.

The effect of MPL was clearly shown when comparing BC (commercial MPL) with all of the other GDLs that possessed a self-assembled microporous layer developed for this study. The performances were particularly lower for BC at high current densities (above 1.3 A/cm^2), indicating that water management was less efficient than self-assembled MPL. Changes in carbon types, hydrophobic agent contents, or porosity between both MPLs could explain this difference.

Polarization curves also indicated that the GDL with 5 wt % PTFE (BA/MPL) and the grafted 1CF3 demonstrate similar performances. The performance of AA-2CF3 is slightly higher than the other GDLs. The grafting of a phenyl group with two hydrophobic CF3 functions may lead to a better covering of GDL fibers compared to a single CF3 function, which is in agreement with the slightly higher hydrophobic behavior as demonstrated in our contact angle measurements. The reproducibility of 1CF3 grafting was validated with two MEAs, which were prepared and tested with similar results in both cases. We expect the same result would also be obtained with 2CF3 grafting.

Under wet conditions (Figure 11), the polarization curve of AA was not shown because the performance was too low to be represented. The impact of MPL was visible when comparing BA/MPL and BC so we can conclude that commercial MPL performed better under wet operating conditions compared to the self-assembled MPL. Regardless, the grafted GDLs (1CF3 and 2CF3) achieved the best results even outperforming the BC. It can be noted that the change in grafted molecules does not alter the performances of our GDLs. The grafting of one or two CF3 functionalities allowed better water management. We can expect that the breakdown on the carbon surface is more homogeneous than the PTFE treatment, as was demonstrated by the XPS mapping for surface distribution. Since the GDL is totally wet at the beginning of the grafting process, it could be expected that the grafted molecules will be bonded onto all the fibers, thus indicating homogeneity across the thickness of the GDL.

In dry conditions (Figure 12), AA/MPL showed the lowest performance, indicating once again that hydrophobic treatment of GDLs is necessary. The polarization curve variation indicated that the 1CF3 grafting onto AA is not suitable for this specific operating condition. The results showed higher resistances for the entire current range, and mass transport limitations were more pronounced than BA/MPL or BC. However, the GDL BC performances remained better than BA/MPL, indicating that commercial MPLs are more suitable for dry conditions. The AA-2CF3 showed the best performances, even better than the BC, indicating that the refined tuning of GDL hydrophobization can lead to a significant increase in the performance even in relatively dry conditions. This is surprising considering a simple reasoning based on water saturation in the GDL at the cathode. However, fuel cell operation results from a complex interplay between transport and electrochemical phenomena occurring at both the cathode and anode, with large in-plane and through-plane heterogeneities in local operation and operating conditions. Water and current distributions in particular vary strongly between humidified and dry conditions from anode to cathode and from rib to channel.[72,73] Further experiments and advanced modeling are required to fully understand this result. Predicting the effect of

DOI: 10.1021/acsami.5b04428
ACS Appl. Mater. Interfaces 2015, 7, 15068−15077

the properties of a component, especially GDL material, on the behavior of a fuel cell is still not straightforward.

Table 3 gives a summary of maximum performances obtained with all testing conditions. Our research suggests that 2CF3 grafting is the best candidate as it showed the best performances for all operating conditions. AA-2CF3/MPL showed an increase of maximum power density of 2.5, 33.9 and 11.3% compared with BA/MPL for automotive, wet, and dry operating conditions, respectively.

Table 3. Maximum Fuel Cell Performance (W/cm^2) of Different GDLs under Automotive, Wet, and Dry Operating Conditions

GDL	80 °C; 50 RH	60 °C; 100 RH	80 °C; 20 RH
AA/MPL	0.41	N/A	0.26
AA-1CF3/MPL	0.78	0.79	0.46
AA-2CF3/MPL	0.80	0.79	0.59
BA/MPL	0.78	0.59	0.53
BC	0.70	0.66	0.56

Complementary research should be performed with the modification of only one electrode at a time to separate the individual contributions of the anode and cathode, as opposed to our study in which both GDLs were modified with the same treatment.

These configurations of grafting enabled us to meet the optimum content of hydrophobic agents in GDL. Lim et al.[12] reported that higher power densities have been obtained with 10 wt % FEP in GDL compared to a 30 wt % under all tested humidification conditions. This optimum should also depend on the nature of the hydrophobic agent. In the case of polymer-treated GDLs, some of the pores are progressively blocked as the polymer content increases in the GDL. With a limited number of anchoring sites for grafting, two 2CF3 molecules might better cover onto the carbon surface due to steric interactions, which would lead to a higher hydrophobic behavior.

4. CONCLUSION

In this study we reported on the first realization of a hydrophobic treatment of GDL by using an electrochemical surface grafting of diazonium salt. The feasibility of our claim has been studied and optimized first onto glassy carbon electrode. The procedure was next applied to commercial GDLs with two types of diazonium salts containing hydrophobic groups, 1CF3 and 2CF3. The grafting was confirmed based on a coupled electrochemical and physicochemical characterization. The XPS core level spectra and mapping showed a successful grafting route, with a homogeneous distribution of the covalently bonded hydrophobic molecules onto the surface of the GDL fibers. According to the modification process, it could be expected that the grafting is homogeneous across the thickness of the GDLs. This result was corroborated by contact angle measurements, showing similar contact angle at the surface of our grafted GDL and polymer modified GDL, both giving rise to superhydrophobic GDLs. The electrochemical modified GDLs were tested in MEA within automotive, wet, and dry conditions, demonstrating better performance compared to the classical route of GDL modification.

AUTHOR INFORMATION

Corresponding Authors

*E-mail: Yohann.THOMAS@cea.fr.

*E-mail: Anass.BENAYAD@cea.fr.

Author Contributions

All authors have given approval to the final version of the manuscript.

Notes

The authors declare no competing financial interest.

ACKNOWLEDGMENTS

The authors acknowledge the funding from the European Union's Seventh Framework Program (FP7/2007-2013) for Fuel Cell and Hydrogen Joint Technology Initiative (IMPALA project, GA 303446) and also the support of the IMPACT Project (GA 303452) for some material characterizations. The collaboration of C. Gas is gratefully acknowledged.

REFERENCES

(1) Li, H.; Tang, Y.; Wang, Z.; Shi, Z.; Wu, S.; Song, D.; Zhang, J.; Fatih, K.; Zhang, J.; Wang, H.; Liu, Z.; Abouatallah, R.; Mazza, A. A Review of Water Flooding Issues in the Proton Exchange Membrane Fuel Cell. *J. Power Sources* **2008**, *178*, 103−117.

(2) Peighambardoust, S. J.; Rowshanzamir, S.; Amjadi, M. Review of the Proton Exchange Membranes for Fuel Cell Applications. *Int. J. Hydrogen Energy* **2010**, *35* (17), 9349−9384.

(3) Sinha, P. K.; Mukherjee, P. P.; Wang, C.-Y. Impact of GDL Structure and Wettability on Water Management in Polymer Electrolyte Fuel Cells. *J. Mater. Chem.* **2007**, *17*, 3089−3103.

(4) Pasaogullari, U.; Wang, C. Y. Liquid Water Transport in Gas Diffusion Layer of Polymer Electrolyte Fuel Cells. *J. Electrochem. Soc.* **2004**, *151* (3), A399−A406.

(5) Park, S.; Lee, J. W.; Popov, B. N. A Review of Gas Diffusion Layer in PEM Fuel Cells: Materials and Designs. *Int. J. Hydrogen Energy* **2012**, *37*, 5850−5865.

(6) Pai, Y. H.; Ke, J. H.; Huang, H. F.; Lee, C. M.; Zen, J.-M.; Shieu, F. S. CF4 Plasma Treatment for Preparing Gas Diffusion Layers in Membrane Electrode Assemblies. *J. Power Sources* **2006**, *161*, 275−281.

(7) Latorrata, S.; Gallo Stampino, P.; Cristiani, C.; Dotelli, G. Novel Superhydrophobic Microporous Layers for Enhanced Performance and Efficient Water Management in PEM Fuel Cells. *Int. J. Hydrogen Energy* **2014**, *39*, 5350−5357.

(8) Gallo Stampino, P.; Latorrata, S.; Molina, D.; Turri, S.; Levi, M.; Dotelli, G. Investigation of Hydrophobic Treatments with Perfluoropolyether Derivatives of Gas Diffusion Layers by Electrochemical Impedance Spectroscopy in PEM-FC. *Solid State Ionics* **2012**, *216*, 100−104.

(9) Gola, M.; Sansotera, M.; Navarrini, W.; Bianchi, C. L.; Gallo Stampino, P.; Latorrata, S.; Dotelli, G. Perfluoropolyether-Functionalized Gas Diffusion Layers for Proton Exchange Membrane Fuel Cells. *J. Power Sources* **2014**, *258*, 351−355.

(10) Park, S.; Kim, S.; Park, Y.; Oh, M. Fabrication of GDL Microporous Layer using PVDF for PEMFCs. *J. Phys.: Conf. Ser.* **2009**, *165*, 012046.

(11) Cabasso, I.; Yuan, Y.; Xu, X. Gas Diffusion Electrodes Based on Poly(vinylidene fluoride) Carbon Blends. U.S. Patent 5,783,325, 1998.

(12) Lim, C.; Wang, C. Y. Effects of Hydrophobic Polymer Content in GDL on Power Performance of a PEM Fuel Cell. *Electrochim. Acta* **2004**, *49*, 4149−4156.

(13) Park, S. B.; Park, Y. Fabrication of Gas Diffusion Layer (GDL) Containing Microporous Layer Using Flourinated Ethylene Prophylene (FEP) for Proton Exchange Membrane Fuel Cell (PEMFC). *Int. J. Precis. Eng. Manuf.* **2012**, *13*, 1145−1151.

(14) Ko, T.-J.; Kim, S. H.; Hong, B. K.; Lee, K.-R.; Oh, K. H.; Moon, M.-W. High Performance Gas Diffusion Layer with Hydrophobic

DOI: 10.1021/acsami.5b04428
ACS Appl. Mater. Interfaces 2015, 7, 15068−15077

Nanolayer under a Supersaturated Operation Condition for Fuel Cells. *ACS Appl. Mater. Interfaces* **2015**, *7*, 5506−5513.
(15) Macleod, E. N. Wet Proofed Conductive Current Collector for the Electrochemical Cells. U.S. Patent 4,215,183, 1980.
(16) Giorgi, L.; Antolini, E.; Pozio, A.; Passalacqua, E. Influence of the PTFE Content in the Diffusion Layer of Low-Pt Loading Electrodes for Polymer Electrolyte Fuel Cells. *Electrochim. Acta* **1998**, *43*, 3675−80.
(17) Bevers, D.; Rogers, R.; von Bradke, M. Examination of the Influence of PTFE Coating on the Properties of Carbon Paper in Polymer Electrolyte Fuel Cells. *J. Power Sources* **1996**, *63*, 193−201.
(18) Park, G. G.; Sohn, Y. J.; Yang, T. H.; Yoon, Y.-G.; Lee, W.-Y.; Kim, C.-S. Effect of PTFE Contents in the Gas Diffusion Media on the Performance of PEMFC. *J. Power Sources* **2004**, *131*, 182−187.
(19) Velayutham, G.; Kaushik, J.; Rajalakshmi, N.; Dhathathreyan, K. S. Effect of PTFE Content in Gas Diffusion Media and Microlayer on the Performance of PEMFC Tested under Ambient Pressure. *Fuel Cells* **2007**, *7*, 314−318.
(20) Ismail, M. S.; Damjanovic, T.; Ingham, D. B.; Ma, L.; Pourkashanian, M. Effect of Polytetrafluoroethylene-Treatment and Microporous Layer-Coating on the in-Plane Permeability of Gas Diffusion Layers Used in Proton Exchange Membrane Fuel Cells. *J. Power Sources* **2010**, *195*, 6619−6628.
(21) Mortazavi, M.; Tajiri, K. Effect of the PTFE Content in the Gas Diffusion Layer on Water Transport in Polymer Electrolyte Fuel Cells (PEFCs). *J. Power Sources* **2014**, *245*, 236−244.
(22) El-kharouf, A.; Mason, T. J.; Brett, D. J. L.; Pollet, B. G. Ex-Situ Characterization of Gas Diffusion Layers for Proton Exchange Membrane Fuel Cells. *J. Power Sources* **2012**, *218*, 393−404.
(23) Wilkinson, D. P.; Zhang, J.; Hui, R.; Fergus, J.; Li, X. *Proton Exchange Membrane Fuel Cell, Materials Properties and Performance*; CRC Press: Boca Raton, FL, 2010, 198−201.
(24) Sinha, P. K.; Wang, C.-Y. Liquid Water Transport in a Mixed-wet Gas Diffusion Layer of a Polymer Electrolyte Fuel Cell. *Chem. Eng. Sci.* **2008**, *63*, 1081−1091.
(25) Kuttanikkad, S. P.; Prat, M.; Pauchet, J. Pore-Network Simulations of Two-Phase Flow in a Thin Porous Layer of Mixed Wettability: Application to Water Transport in Gas Diffusion Layers of Proton Exchange Membrane Fuel Cells. *J. Power Sources* **2011**, *196*, 1145−1155.
(26) Pauchet, J.; Prat, M.; Schott, P.; Kuttanikkad, S. P. Performance Loss of Proton Exchange Membrane Fuel Cell due to Hydrophobicity Loss in Gas Diffusion Layer: Analysis by Multiscale Approach Combining Pore Network and Performance Modelling. *Int. J. Hydrogen Energy* **2012**, *37*, 1628−1641.
(27) Park, S.; Lee, J. W.; Popov, B. N. Effect of PTFE Content in Microporous Layer on Water Management in PEM Fuel Cells. *J. Power Sources* **2008**, *177*, 457−463.
(28) Das, P. K.; Grippin, A.; Kwong, A.; Weber, A. Liquid-Water-Droplet Adhesion-Force Measurements on Fresh and Aged Fuel-Cell Gas-Diffusion Layers. *J. Electrochem. Soc.* **2012**, *159*, B489−B496.
(29) Zhou, P.; Wu, C. W. Liquid Water Transport Mechanism in the Gas Diffusion Layer. *J. Power Sources* **2010**, *195* (5), 1408−1415.
(30) Rofaiel, A.; Ellis, J. S.; Challa, P. R.; Bazylak, A. Heterogeneous Through-Plane Distributions of Polytetrafluoroethylene in Polymer Electrolyte Membrane Fuel Cell Gas Diffusion Layers. *J. Power Sources* **2012**, *201*, 219−225.
(31) Ito, H.; Abe, K.; Ishida, M.; Nakano, A.; Maeda, T.; Munakata, T.; Nakajima, H.; Kitahara, T. Effect of Through-Plane Distribution of Polytetrafluoroethylene in Carbon Paper on in-Plane Gas Permeability. *J. Power Sources* **2014**, *248*, 822−830.
(32) Molaeimanesh, G. R.; Akbari, M. H. Impact of PTFE Distribution on the Removal of Liquid Water from a PEMFC Electrode by Lattice Boltzmann Method. *Int. J. Hydrogen Energy* **2014**, *39*, 8401−8409.
(33) Assresahegn, B. D.; Brousse, T.; Bélanger, D. Advances on the use of Diazonium Chemistry for Functionalization of Materials Used in Energy Storage Systems. *Carbon* **2015**, *92*, 362−381.
(34) Le, X. T.; Viel, P.; Jégou, P.; Garcia, A.; Berthelot, T.; Bui, T. H.; Palacin, S. Diazoniuminduced Anchoring Process: An Application To Improve the Monovalent Selectivity of Cation Exchange Membranes. *J. Mater. Chem.* **2010**, *20*, 3750−3757.
(35) Adenier, A.; Cabet-Deliry, E.; Chaussé, A.; Griveau, S.; Mercier, F.; Pinson, J.; Vautrin-Ul, C. Grafting of Nitrophenyl Groups on Carbon and Metallic Surfaces without Electrochemical Induction. *Chem. Mater.* **2005**, *17*, 491−501.
(36) Combellas, C.; Delamar, M.; Kanoufi, F.; Pinson, J.; Podvorica, F. I. Spontaneous Grafting of Iron Surfaces by Reduction of Aryldiazonium Salts in Acidic or Neutral Aqueous Solution. Application to the Protection of Iron against Corrosion. *Chem. Mater.* **2005**, *17*, 3968−3975.
(37) Chaussé, A.; Chehimi, M. M.; Karsi, N.; Pinson, J.; Podvorica, F.; Vautrin-Ul, C. The Electrochemical Reduction of Diazonium Salts on Iron Electrodes. The Formation of Covalently Bonded Organic Layers and Their Effect on Corrosion. *Chem. Mater.* **2002**, *14*, 392−400.
(38) Lyskawa, J.; Bélanger, D. Direct Modification of a Gold Electrode with Aminophenyl Groups by Electrochemical Reduction of in Situ Generated Aminophenyl Monodiazonium Cations. *Chem. Mater.* **2006**, *18*, 4755−4763.
(39) Mévellec, V.; Roussel, S.; Tessier, L.; Chancolon, J.; Mayne-L'Hermite, M.; Deniau, G.; Viel, P.; Palacin, S. Grafting Polymers on Surfaces: A New Powerful and Versatile Diazonium Salt-Based One-Step Process in Aqueous Media. *Chem. Mater.* **2007**, *19*, 6323−6330.
(40) Liu, G.; Böcking, T.; Gooding, J. Diazonium Salts: Stable Monolayers on Gold Electrodes for Sensing Applications. *J. Electroanal. Chem.* **2007**, *600* (2), 335−344.
(41) Bahr, J. L.; Tour, J. M. Highly Functionalized Carbon Nanotubes Using in Situ Generated Diazonium Compounds. *Chem. Mater.* **2001**, *13*, 3823−3824.
(42) Weissmann, M.; Baranton, S.; Clacens, J.-M; Coutanceau, C. Modification of Hydrophobic/Hydrophilic Properties of Vulcan XC72 Carbon Powder by Grafting of Trifluoromethylphenyl and Phenylsulfonic Acid Groups. *Carbon* **2010**, *48*, 2755−2764.
(43) Wang, X.; Liu, R.; Waje, M. M.; Chen, Z.; Yan, Y.; Bozhilov, K. N.; Feng, P. Sulfonated Ordered Mesoporous Carbon as a Stable and Highly Active Protonic Acid Catalyst. *Chem. Mater.* **2007**, *19*, 2395−2397.
(44) Jung, N.; Kim, S. M.; Kang, D. H.; Chung, D. Y.; Kang, Y. S.; Chung, Y.-H.; Choi, Y. W.; Pang, C.; Suh, K.-Y.; Sung, Y. E. High-Performance Hybrid Catalyst with Selectively Functionalized Carbon by Temperature-Directed Switchable Polymer. *Chem. Mater.* **2013**, *25*, 1526−1532.
(45) Seck, S. M.; Charvet, S.; Fall, M.; Baudrin, E.; Geneste, F.; Lejeune, M.; Benlahsen, M. Functionalization of Amorphous Nitrogenated Carbon Thin Film Electrodes for Improved Detection of Cadmium vs. Copper Cations. *J. Electroanal. Chem.* **2015**, *738*, 154−161.
(46) Gao, W.; Majumder, M.; Alemany, L. B.; Narayanan, T. N.; Ibarra, M. A.; Pradhan, B. K.; Ajayan, P. M. Engineered Graphite Oxide Materials for Application in Water Purification. *ACS Appl. Mater. Interfaces* **2011**, *3*, 1821−1826.
(47) Kariuki, J. K.; McDermott, M. T. Nucleation and Growth of Functionalized Aryl Films on Graphite Electrodes. *Langmuir* **1999**, *15*, 6534−6540.
(48) Coulon, E.; Pinson, J.; Bourzat, J.-D.; Commerçon, A.; Pulicani, J. P. Electrochemical Attachment of Organic Groups to Carbon Felt Surfaces. *Langmuir* **2001**, *17*, 7102−7106.
(49) Chehimi, M. M.; Lamouri, A.; Picot, M.; Pinson, J. Surface Modification of Polymers by Reduction of Diazonium Salts: Polymethylmethacrylate as an Example. *J. Mater. Chem. C* **2014**, *2*, 356−363.
(50) Menanteau, T.; Levillain, E.; Breton, T. Electrografting via Diazonium Chemistry: From Multilayer to Monolayer Using Radical Scavenger. *Chem. Mater.* **2013**, *25* (14), 2905−2909.
(51) Pandurangappa, M.; Lawrence, N. S.; Compton, R. G. Homogeneous Chemical Derivatisation of Carbon Particles: A Novel

DOI: 10.1021/acsami.5b04428
ACS Appl. Mater. Interfaces 2015, 7, 15068−15077

Method for Funtionalising Carbon Surfaces. *Analyst* **2002**, *127*, 1568−1571.
(52) Lamberti, F.; Agnoli, S.; Brigo, L.; Granozzi, G.; Giomo, M.; Elvassore, N. Surface Functionalization of Fluorine-Doped Tin Oxide Samples through Electrochemical Grafting. *ACS Appl. Mater. Interfaces* **2013**, *5*, 12887−12894.
(53) Flavel, B. S.; Gross, A. J.; Garrett, D. J.; Nock, V.; Downard, A. J. A Simple Approach to Patterned Protein Immobilization on Silicon via Electrografting from Diazonium Salt Solutions. *ACS Appl. Mater. Interfaces* **2010**, *2*, 1184−1190.
(54) Simons, B. M.; Lehr, J.; Garrett, D. J.; Downard, A. Formation of Thick Aminophenyl Films from Aminobenzenediazonium Ion in the Absence of a Reduction Source. J. *Langmuir* **2014**, *30* (17), 4989−4996.
(55) Breton, T.; Bélanger, D. Modification of Carbon Electrode with Aryl Groups Having an Aliphatic Amine by Electrochemical Reduction of in Situ Generated Diazonium Cations. *Langmuir* **2008**, *24*, 8711−8718.
(56) Bell, K. J.; Brooksby, P. A.; Polson, M. I. J.; Downard, A. Evidence for Covalent Bonding of Aryl Groups to MnO_2 Nanorods from Diazonium-Based Grafting. *Chem. Commun.* **2014**, *50*, 13687−13690.
(57) Delaporte, N.; Perea, A.; Amin, R.; Zaghib, K.; Bélanger, D. Chemically Grafted Carbon-Coated $LiFePO_4$ using Diazonium Chemistry. *J. Power Sources* **2015**, *280*, 246−255.
(58) Baranton, S.; Bélanger, D. Electrochemical Derivatization of Carbon Surface by Reduction of in situ Generated Diazonium Cations. *J. Phys. Chem. B* **2005**, *109* (51), 24401−24410.
(59) Bélanger, D.; Pinson, J. Electrografting: A Powerful Method for Surface Modification. *Chem. Soc. Rev.* **2011**, *40*, 3995−4048.
(60) Pinson, J. Attachment of Organic Layers to Materials Surfaces by Reduction of Diazonium Salts. In *Aryl Diazonium Salts*; Wiley-VCH Verlag GmbH & Co. KGaA: Weinheim, Germany, 2012, 1−35.
(61) Delamar, M.; Hitmi, R.; Pinson, J.; Saveant, J., M. Covalent Modification of Carbon Surfaces by Grafting of Functionalized Aryl Radicals Produced from Electrochemical Reduction of Diazonium Salts. *J. Am. Chem. Soc.* **1992**, *114*, 5883−5884.
(62) Allongue, P.; Delamar, M.; Desbat, B.; Fagebaume, O.; Hitmi, R.; Pinson, J.; Saveant, J.-M. Covalent Modification of Carbon Surfaces by Aryl Radicals Generated from the Electrochemical Reduction of Diazonium Salts. *J. Am. Chem. Soc.* **1997**, *119*, 201−207.
(63) Granger, M. C.; Swain, G. M. The Influence of Surface Interactions on the Reversibility of Ferri/Ferrocyanide at Boron-Doped Diamond Thin-Film Electrodes. *J. Electrochem. Soc.* **1999**, *146* (12), 4551−4558.
(64) Gurau, V.; Bluemle, M. J.; De Castro, E. S.; Tsou, Y.-M.; Mann, J. A., Jr.; Zawodzinski, T. A., Jr. Characterization of Transport Properties in Gas Diffusion Layers for Proton Exchange Membrane Fuel Cells. 1. Wettability (Internal Contact Angle to Water and Surface Energy of GDL Fibers). *J. Power Sources* **2006**, *160*, 1156−1162.
(65) Starov, V. M.; Kosvintsev, S. R.; Velarde, M. G. Spreading of Surfactant Solutions over Hydrophobic Substrates. *J. Colloid Interface Sci.* **2000**, *227* (1), 185−190.
(66) Vazquez, G.; Alvarez, E.; Navaza, J. M. Surface Tension of Alcohol + Water from 20 to 50°C. *J. Chem. Eng. Data* **1995**, *40* (3), 611−614.
(67) Owen, M. J. Surface Tension of Polytrifluoropropylmethylsiloxane. *J. Appl. Polym. Sci.* **1988**, *35* (4), 895−901.
(68) Thomas, Y. R. J.; Bruno, M. M.; Corti, H. R. Characterization of a Monolithic Mesoporous Carbon as Diffusion Layer for Micro Fuel Cells Application. *Microporous Mesoporous Mater.* **2012**, *155*, 47−55.
(69) Benayad, A.; Li, X. S. Carbon Free Nickel Subsurface Layer Tessellating Graphene on Ni(111) Surface. *J. Phys. Chem. C* **2013**, *117*, 4727−4733.
(70) Benayad, A.; Shin, H. J.; Park, H. K.; Yoon, S. M.; Kim, K. K.; Jin, M. H.; Jeong, H. K.; Lee, J. C.; Choi, J. Y.; Lee, Y. H. Controlling Work Function of Reduced Graphite Oxide with Au-Ion Concentration. *Chem. Phys. Lett.* **2009**, *475*, 91−95.
(71) Moulder, J. F.; Stickle, W. F.; Sobol, P. E.; Bomben, K. D. *Handbook of X-ray Photoelectron Spectroscopy*; Physical Electronics, Inc.: Eden Prairie, MN, 1995.
(72) Reum, M.; Freunberger, S. A.; Wokaun, A.; Büchi, F. N. Measuring the Current Distribution with Submillimeter Resolution in PEFCs: II. Impact of Operating Parameters. *J. Electrochem. Soc.* **2009**, *156* (3), B301−B310.
(73) Oberholzer, P.; Boillat, P. Local Characterization of PEFCs by Differential Cells: Systematic Variations of Current and Asymmetric Relative Humidity. *J. Electrochem. Soc.* **2014**, *161* (1), F139−F152.

DOI: 10.1021/acsami.5b04428
ACS Appl. Mater. Interfaces 2015, 7, 15068−15077